Intense-Field Alignment of Molecules Confined in Octahedral Fields

Toni Kiljunen,[1] Burkhard Schmidt,[2] and Nikolaus Schwentner[1,*]

[1]*Institut für Experimentalphysik, Freie Universität Berlin, Arnimallee 14, D-14195 Berlin, Germany*

[2]*Institut für Mathematik II, Freie Universität Berlin, Arnimallee 2-6, D-14195 Berlin, Germany*

(Received 3 November 2004; published 30 March 2005)

The combined effect of static octahedral potential and anisotropic interactions with intense linearly polarized light on the rotational motion of linear molecules is investigated. Avoided crossings of quantized energy levels corresponding to pendular states with different degrees of alignment are found by varying the strength parameters for the light and static fields. High alignment is achieved for both cooperative and competitive choices of the relative directionality of the two fields, thus presenting means for controlling the dynamics of impurity centers with respect to the surrounding media.

DOI: 10.1103/PhysRevLett.94.123003 PACS numbers: 33.80.-b, 42.50.Vk, 71.70.Ch, 82.50.-m

Librational states of molecules embedded in solids represent a well established concept [1–4] to describe their hindered rotational motion. The directional manipulation of molecular impurities by external fields is a hitherto unexplored field. This problem is approached by applying the methodology developed [5] for the laser-induced alignment of free molecules to the crystal field case. The goal of achieving alignment of molecules confined in crystal fields can be cast into two fundamental cases. Case **A** consists of creating alignment along one of the directions preferred by the crystal field. In the more challenging case **B**, the possibility of aligning a molecule in an unfavorable direction is investigated, thus turning the molecular axis away from the natural directions provided by the crystal. In this Letter, the degree of alignment, the energetics, and especially the avoided curve crossings are derived for different crystal field states versus the strength parameter of the laser field in order to lay the grounds for future dynamical calculations.

We study locally octahedral (O_h) symmetry appearing, for example, at a substitutional or interstitial site in a fcc lattice. Such a situation is realized, e.g., for molecules embedded in solid rare gases [6], alkali halides [7,8], or fullerites [9,10]. The ranges of crystal field and laser strength parameters cover those relevant for small molecules in rare gas crystals [11,12] for which alignment experiments are underway. Particularly, the goal is to control the yield of bond breaking and subsequent reaction mechanisms [13]. To provide insight into the fundamental conditions of alignment, we restrict ourselves to a linear guest molecule. In the gas phase, alignment can be achieved by an intense, nonresonant laser field. The interaction with the induced dipole due to anisotropic polarizability converts free rotational motion into small-amplitude libration [14]. The resulting pendular states can be further narrowed by the use of tailored pulse sequences [15–17], and addition of a static field enables even orientation [18,19].

The quantum mechanical Hamiltonian for a confined linear rotor with angular momentum J is given by

$$\hat{H}/B = \hat{\mathbf{J}}^2 + \hat{V}_\alpha + \hat{V}_\kappa \tag{1}$$

in units of rotational constant $B = \hbar^2/(2I)$ with moment of inertia I. Upon averaging over the optical cycles, the light-induced potential is obtained as [14]

$$V_\alpha = -(\Delta\omega\cos^2\theta' + \omega_\perp), \tag{2}$$

where the dimensionless parameter $\Delta\omega = \mathcal{E}^2\Delta\alpha/(4B)$ describes the interaction of a field $\mathcal{E}$ with an anisotropic polarizability ($\Delta\alpha = \alpha_\parallel - \alpha_\perp$), where the components ($\parallel$, $\perp$) refer to the particle's axis, and where θ' is the angle with the polarization direction. The time-independent rotational Schrödinger equation is solved in the basis set of symmetry adapted spherical harmonics (SASH) [20,21]. The static interaction potential V_κ is expanded in terms of the two lowest order A_{1g} SASH of the O_h group:

$$\begin{aligned} V_\kappa &= \kappa(K_4 V_4 + K_6 V_6) \\ V_4 &= \sqrt{7/12}Y_{4,0} + \sqrt{5/24}(Y_{4,4} + Y_{4,-4}) \\ V_6 &= \sqrt{1/8}Y_{6,0} - \sqrt{7/16}(Y_{6,4} + Y_{6,-4}), \end{aligned} \tag{3}$$

where κ is a strength parameter and $Y_{J,M}(\theta, \phi)$ are spherical harmonics. Including the effect of the laser field, with linear polarization along a fourfold (C_4) symmetry axis of the static field ($\theta = \theta'$), reduces the overall symmetry to the D_{4h} subgroup [22].

Equation (3) allows us to vary potential shapes with the interactions along fourfold (C_4), threefold (C_3), or twofold (C_2) symmetry axes chosen repulsive or attractive relative to each other [4]. For brevity, we consider two prototypical situations. Potential **A** ($K_4 = -1.1252$, $K_6 = -0.7584$) has one set of minima with $V_\kappa/\kappa = -1(\theta = 0, \pi)$ coinciding with the polarization direction; see Fig. 1. The C_3 directions give the energy zero (local minimum), and maxima are found along the C_2 axes with $V_{\kappa,\max}/\kappa = 0.6250$. Hence the potential supports the target state of the alignment field, and high degree of alignment is expected because the two fields are partially (at $\theta = 0, \pi$) *cooperative*. Potential **B** ($K_4 = 0.6329$, $K_6 = -1.1376$)

represents a contrary case where the characters of the three and fourfold directions are interchanged and $V_{\kappa,\max}/\kappa = 0.5625$. Now, the potential minima with $V_\kappa/\kappa = -1$ are off the alignment directions at $\theta = 0, \pi$ by $\cos^{-1}(1/\sqrt{3})$. A potential barrier needs to be overcome to achieve significant alignment along the field, thus representing a *competitive* case.

The calculated energy spectra for the crystal field alone, $E_n(\kappa; V_\alpha = 0)$ shown in Fig. 2, illustrate the transition from a free rotor ($\kappa = 0$) to a hindered case, where the rotational motion is confined to small-amplitude libration about the minimum energy directions of the **A** and **B** potentials. For increasing the interaction strength κ, the lowest energy levels begin to coalesce into *near-degenerate* sets. At $\kappa = 50$, for case **A** the lowest of these sets comprises of A_{1g}, T_{1u}, and E_g states correlating with a sixfold degenerate librational ground state in the limit of $\kappa \to \infty$. In case **B**, the A_{1g}, T_{1u}, T_{2g}, and A_{2u} states are close to the eightfold degenerate ground state for the librator limit; see also the inserts of Fig. 2. The rotational densities for $\kappa = 50$ are already relatively well aligned with respect to the six (C_4) or eight (C_3) minima supported by the two potentials, respectively. At $\kappa = 100$, the next 12 (**A**) and 16 (**B**) states are close to the first excited state of the librator limit, while considerably stronger crystal fields are necessary to bring the higher states close to that limit. We note that the energy level scheme in the limit $\kappa \to \infty$ remains anharmonic.

The zero-point energy in these potentials is more than half of the potential well depth $V_{\kappa,\min} = -\kappa$ (lower dashed lines in Fig. 2), thereby significantly reducing the effective barrier for alignment. There are relatively few states below the maximum of the potential energy; see upper dashed lines. For $\kappa = 50$, those are 30 states for both **A** and **B**. We note that the considerable extent of the zero-point energies limits classical approaches in estimating the rotational barriers and densities.

In the following we study the aspect of alignment by V_α for fixed crystal field V_κ. We restrict ourselves to the case

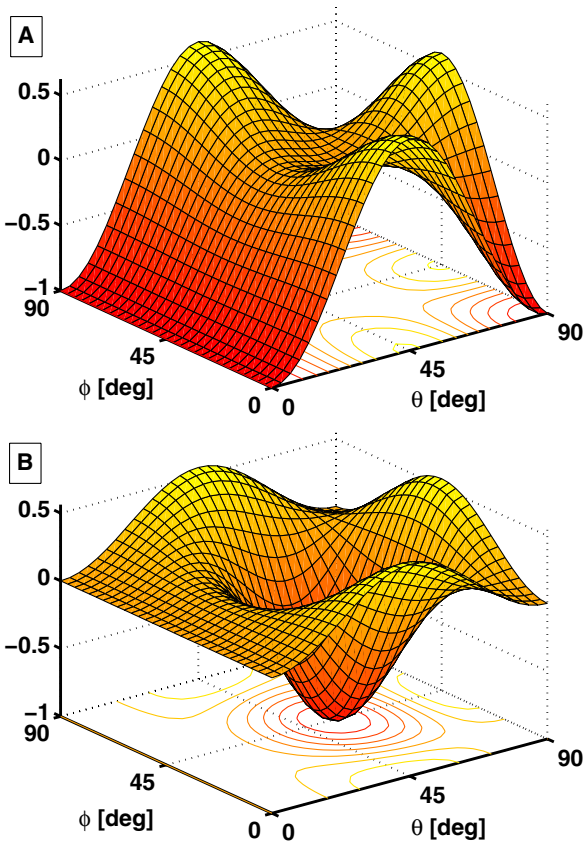

FIG. 1 (color online). Octahedral interaction potentials $V_\kappa(\theta, \phi)/\kappa$. Cases **A** and **B** (minima along fourfold and threefold axes of symmetry, respectively) represent cooperative and competitive arrangements with respect of alignment along $\theta = 0, 180°$. Shown is one octant $[0, \pi/2]$.

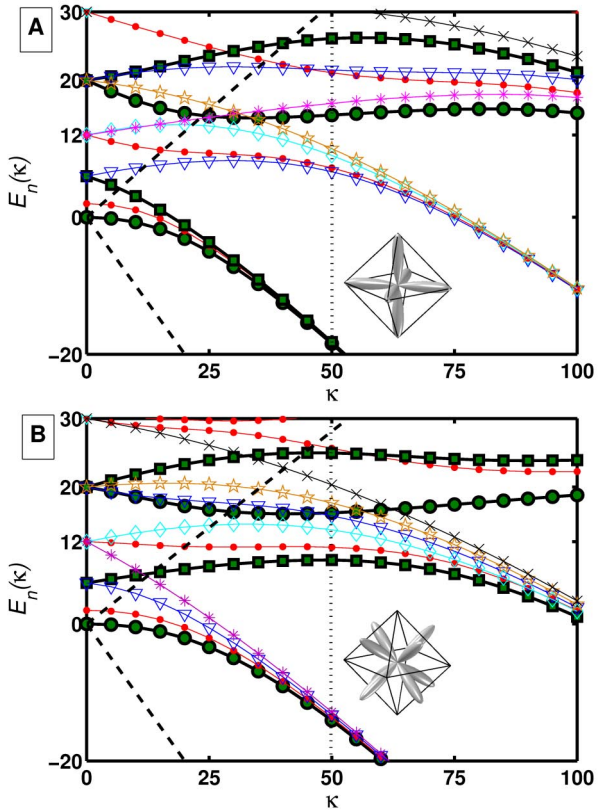

FIG. 2 (color online). Dependence of the energy spectrum $E_n(\kappa; V_\alpha = 0)$ on the interaction strength parameter κ for potentials **A** and **B**. The symbols are chosen according to irreducible representations of the O_h point group: A_{1g} (circles), T_{1u} (points), E_g (squares), T_{2g} (triangles), T_{2u} (diamonds), A_{2u} (asterisks), T_{1g} (five-pointed stars), and E_u (crosses). The dashed lines indicate the minimum $V_\kappa = -\kappa$ and maximum of the potential energy. The vertical dotted line locates the $\kappa = 50$ cut used later in the discussion. The A_{1g} ground state rotational density at $\kappa = 50$ is drawn in the octahedra.

of $\kappa = 50$ where the potential wells are deep enough to support directional states while the energy spectrum is still sufficiently far from that of the librational limit, thus representing typical crystal fields [8] and matrix-isolation applications [12].

Without loss of generality, we study only the lowest four totally symmetric states (A_{1g}) of the D_{4h} subgroup. The other representations exhibit qualitatively similar field dependence of the energy spectrum. Note that the A_{1g} representation derives from both A_{1g} and E_g of the original O_h symmetry [22]. The four states studied here stem from the two A_{1g} and two E_g curves of the O_h group emphasized in Fig. 2.

Optically dressed energy levels $E_n(\Delta\omega; \kappa = 50)$ for the combined action of the static and the light-induced potentials are shown in Fig. 3. We neglect the angle-independent part of V_α in Eq. (2) by setting $\omega_\perp = 0$. In case **A**, the twofold degeneracy of the ground state is lifted as the field is switched on. While one energy level (diamonds) is essentially field insensitive, the ground state (circles), as well as the two upper high-field seeking states, gain energy for $\Delta\omega > 0$. In agreement with the noncrossing rule for states of equal symmetry, this leads to two avoided crossings at $\Delta\omega \approx 60$ and 110, as seen in the upper part of Fig. 3. This different behavior is due to the directionality of the wave functions with their lobes pointing either perpendicular (high M) or increasingly parallel ($M = 0$) to the field; see the inserts in Fig. 3. This is also reflected in Fig. 4, where the expectation values $\langle\cos^2\theta\rangle$ are shown. The high degree of alignment ($> 90\%$) for the parallel ground state exceeds that of the gas phase case [23], while the alignment ($< 10\%$) for the perpendicular state is below the corresponding gas phase value. Also, the pattern of avoided crossings of the energy levels is repeated. The dashed curves give the averaged alignment $\langle\langle\cos^2\theta\rangle\rangle$ for a thermal ensemble without symmetry restrictions. High alignment can be achieved using fairly low intensities ($\Delta\omega \approx 40$) for cryogenic conditions, here $\mathcal{T} = 10\ k_B/B$, as realized in most of the above mentioned experiments. For this temperature, only the states correlated with the sixfold librational ground state are significantly populated.

In case **B** (see lower parts of Figs. 3 and 4), the four states under investigation do not exhibit notable rotational

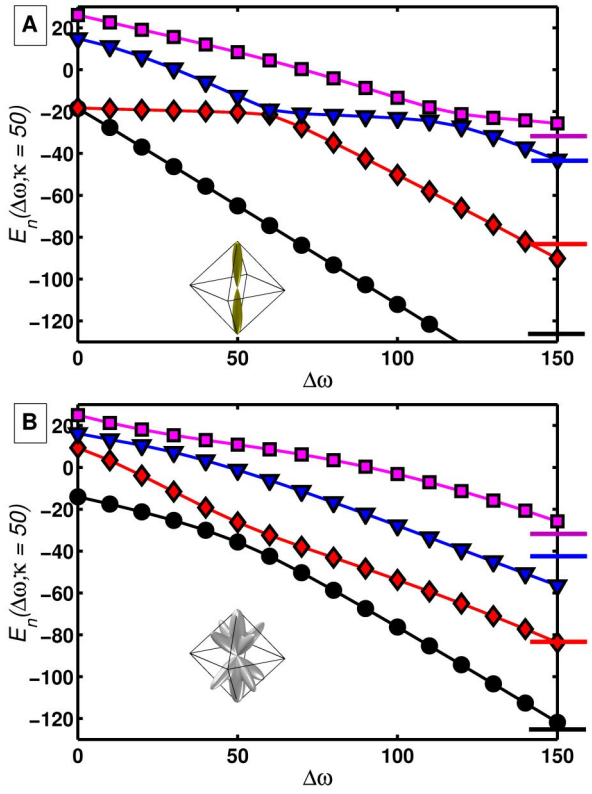

FIG. 3 (color online). Dependence of four lowest energy levels of $A_{1g}(D_{4h})$ symmetry on the alignment field strength ($\Delta\omega$) for fixed static potential ($\kappa = 50$). The horizontal bars on the right-hand side depict the corresponding energy levels at $\Delta\omega = 150$ when $\kappa = 0$. Rotational density of the ground state is displayed in the inserted octahedra at $\Delta\omega = 50$. The $\omega_\perp$ component is set to zero.

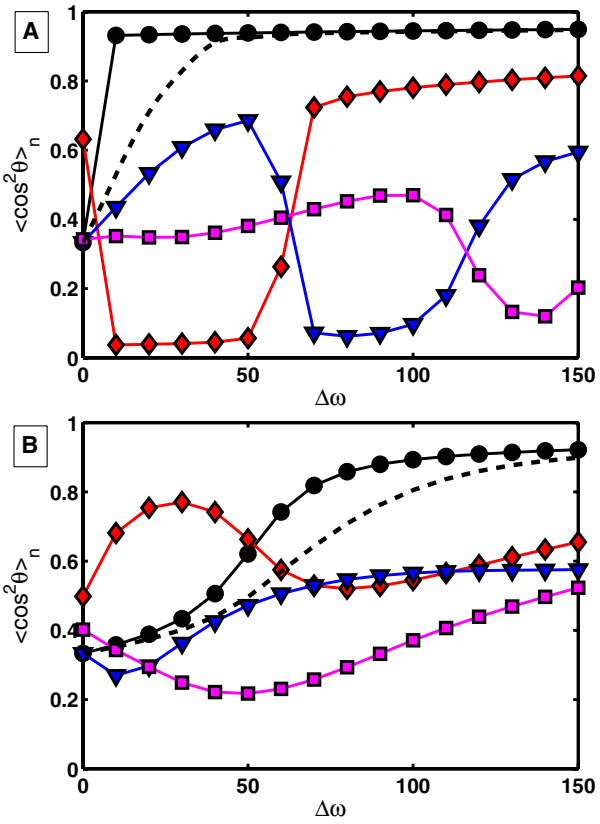

FIG. 4 (color online). The degree of alignment $\langle\cos^2\theta\rangle$ for the four lowest states in A_{1g} representation as the strength parameter $\Delta\omega$ is varied (for constant static field $\kappa = 50$). Same labeling is used as in Fig. 3. The dashed curves show the thermally averaged (considering all D_{4h} representations) alignment for $\mathcal{T} = 10\ k_B/B$.

density parallel to the target C_4 axis for $\Delta\omega = 0$. On the other hand, they have no perpendicular contribution, either. Therefore, the crossings of the energy levels are less pronounced compared to the above case. However, the $\langle\cos^2\theta\rangle$ curves can be used to locate the intersections. Inspecting the wave functions in the absence of the laser field, we find that the target state property [wave function lobes pointing towards $\theta = 0, \pi$ as in insert of Fig. 3(A)] is dominantly present in the fourth eigenstate (squares). In passing the avoided crossings for increasing $\Delta\omega$, this property is first transformed to third (triangles) and second (diamonds) roots. Finally, beyond the crossing at $\Delta\omega \approx 50$, the ground state (circles) as well as the thermal average (dashed) inherit high alignment.

In conclusion, we investigated the alignment effect induced by laser fields for linear molecules subject to static O_h fields. We found cooperative effects for case **A**, where the direction of the field polarization coincides with one of the potential energy minima. Within the reduced D_{4h} symmetry, the ground state density becomes confined to the polarization axis with enhanced alignment, $\langle\cos^2\theta\rangle$ approaching unity already for $\Delta\omega/\kappa \ll 1$. For the competitive case **B**, where the potential minima are at the C_3 directions, a highly aligned ground state, $\langle\cos^2\theta\rangle > 90\%$, was found only for $\Delta\omega/\kappa \gtrsim 2$. This was explained in terms of the avoided crossings between ground and proper excited states. It is expected that these crossings of energy levels play also a central role in designing laser pulses to control molecular processes, where the induced dynamics varies between adiabatic following for pulses long compared to the rotational period $\pi\hbar/B$ and strongly nonadiabatic behavior in the impulsive regime [15,24]. High and durable alignment can be achieved by combinations [25,26] of adiabatic and nonadiabatic passages through the avoided crossings shown here. For instance, the pronounced crossing between second and third energy levels in case **A** is promising because the corresponding states have very different degrees of alignment. A Landau-Zener-Stueckelberg estimate of a transition probability for a linear sweep, based on the static results (gaps and slopes in Fig. 3), shows that nearly adiabatic behavior ($\geq 99\%$) can be realized with $d\Delta\omega/dt < 3B/\hbar$ while almost nonadiabatic passage is found for $d\Delta\omega/dt > 10^3 B/\hbar$. This allows for preparing suitably aligned precursor states to efficiently control subsequent direction-dependent reaction mechanisms. We note the existence of tunneling doublets of librational energy levels possibly allowing even control of molecular orientation [19].

Financial support by the *Deutsche Forschungsgemeinschaft* through program Sfb 450 is gratefully acknowledged. T. K. is supported by Contract No. HPMF-CT-2002-01854.

*Email: nikolaus.schwentner@physik.fu-berlin.de

[1] L. Pauling, Phys. Rev. **36**, 430 (1930).
[2] A. F. Devonshire, Proc. Roy. Soc. (London) **A153**, 601 (1936).
[3] H. U. Beyeler, J. Chem. Phys. **60**, 4123 (1974).
[4] G. K. Pandey, K. L. Pandey, M. Massey, and R. Kumar, Phys. Rev. B **34**, 1277 (1986).
[5] H. Stapelfeldt and T. Seideman, Rev. Mod. Phys. **75**, 543 (2003).
[6] V. A. Apkarian and N. Schwentner, Chem. Rev. **99**, 1481 (1999).
[7] K. Nishidate, M. Baba, Sarjono, M. Hasegawa, K. Nishigawa, I. Sokolska, and R. Ryba-Romanowski, Phys. Rev. B **68**, 224307 (2003).
[8] C. E. Mungan, U. Happek, J. T. McWhirter, and A. J. Sievers, J. Chem. Phys. **107**, 2215 (1997).
[9] T. Yildirim and A. B. Harris, Phys. Rev. B **66**, 214301 (2002).
[10] I. Holleman, G. von Helden, A. van der Avoird, and G. Meijer, Phys. Rev. Lett. **80**, 4899 (1998).
[11] J. Manz, P. Saalfrank, and B. Schmidt, J. Chem. Soc., Faraday Trans. **93**, 957 (1997).
[12] V. Berghof, M. Martins, B. Schmidt, and N. Schwentner, J. Chem. Phys. **116**, 9364 (2002).
[13] T. Kiljunen, M. Bargheer, M. Gühr, N. Schwentner, and B. Schmidt, Phys. Chem. Chem. Phys. **6**, 2932 (2004).
[14] B. Friedrich and D. Herschbach, Phys. Rev. Lett. **74**, 4623 (1995).
[15] M. Leibscher, I. S. Averbukh, and H. Rabitz, Phys. Rev. Lett. **90**, 213001 (2003).
[16] J. Ortigoso, Phys. Rev. Lett. **93**, 073001 (2004).
[17] C. Z. Bisgaard, M. D. Poulsen, E. Péronne, S. S. Viftrup, and H. Stapelfeldt, Phys. Rev. Lett. **92**, 173004 (2004).
[18] H. Sakai, S. Minemoto, H. Nanjo, H. Tanji, and T. Suzuki, Phys. Rev. Lett. **90**, 083001 (2003).
[19] B. Friedrich, N. H. Nahler, and U. Buck, J. Mod. Opt. **50**, 2677 (2003).
[20] C. J. Bradley and A. P. Cracknell, *The Mathematical Theory of Symmetry in Solids* (Clarendon, Oxford, 1972).
[21] B. Schmidt and P. Žďánská, Comput. Phys. Commun. **127**, 290 (2000).
[22] E. B. Wilson, Jr., J. C. Decius, and P. C. Cross, *Molecular Vibrations* (Dover, New York, 1955).
[23] B. Friedrich and D. Herschbach, J. Chem. Phys. **111**, 6157 (1999).
[24] J. Ortigoso, M. Rodríguez, M. Gupta, and B. Friedrich, J. Chem. Phys. **110**, 3870 (1999).
[25] T. Seideman, J. Chem. Phys. **115**, 5965 (2001).
[26] J. G. Underwood, M. Spanner, M. Y. Ivanov, J. Mottershead, B. J. Sussman, and A. Stolow, Phys. Rev. Lett. **90**, 223001 (2003).